Available online at www.sciencedirect.com

ScienceDirect

www.elsevier.com/locate/matchar

Microstructure and mechanical properties of diffusion bonded W/steel joint using V/Ni composite interlayer

W.S. Liu, Q.S. Cai*, Y.Z. Ma, Y.Y. Wang, H.Y. Liu, D.X. Li

State Key Laboratory of Powder Metallurgy, Central South University, Changsha 410083, PR China

ARTICLE DATA

Article history:
Received 23 April 2013
Received in revised form
3 September 2013
Accepted 11 October 2013

Keywords:
Diffusion bonding
Interlayer
Tungsten
Steel
Electron probe microanalysis

ABSTRACT

Diffusion bonding between W and steel using V/Ni composite interlayer was carried out in vacuum at 1050 °C and 10 MPa for 1 h. The microstructural examination and mechanical property evaluation of the joints show that the bonding of W to steel was successful. No intermetallic compound was observed at the steel/Ni and V/W interfaces for the joints bonded. The electron probe microanalysis and X-ray diffraction analysis revealed that Ni_3V, Ni_2V, Ni_2V_3 and NiV_3 were formed at the Ni/V interface. The tensile strength of about 362 MPa was obtained for as-bonded W/steel joint and the failure occurred at W near the V/W interface. The nano-indentation test across the joining interfaces demonstrated the effect of solid solution strengthening and intermetallic compound formation in the diffusion zone.

1. Introduction

In fusion reactors, the divertor components during operation are subjected to high heat flux, high particle flux, and heavy neutron flux. To resist an extremely high heat flux of at least 10 MW/m^2, a helium-cooled high performance divertor concept for demonstration reactor (DEMO) was proposed [1]. According to the design, the targeted development of helium-cooled divertor requires joining tungsten (W) and its alloy to reduced activation ferritic/martensitic steel [2,3]. However, W and steel have significant differences in physical properties, in particular the mismatch of their coefficients of thermal expansion (CTE), which causes high thermal residual stress in the W/steel joints after joining. This results in a reduction in mechanical properties of the joint.

Joining of W to steel by conventional fusion welding is inapplicable because of the large difference in their melting points. Several attempts in brazing of W to steel using rapidly solidified amorphous and microcrystalline foil-type filler metals have been made in recent years [4–6]. Oono et al. [7,8] reported successful brazing of W and ODS steel using an iron-based amorphous alloy. Although brazing alloys are metallurgically compatible with parent materials, the brazing temperature is usually much higher than the recrystallization temperature of the materials (e.g., EUROFER97 [9]) to be joined. In addition, the upper working temperature of the assembly is also compromised by the presence of the lower-melting-point brazing alloy. Diffusion bonding seems to be a suitable way to join W with steel due to its tolerable bonding temperature and the joint can be used at high temperatures. In the case of diffusion bonding of dissimilar materials, an interlayer inserted between substrates is often necessary to prevent the formation of intermetallic compounds and to reduce the residual stress in the joints [10,11]. The current study deals with the diffusion

* *Corresponding author*. Tel.: +86 0731 88877825.
E-mail address: cai2009pm@163.com (Q.S. Cai).

1044-5803/$ – see front matter
http://dx.doi.org/10.1016/j.matchar.2013.10.013

bonding of W to steel using Ni [12,13], Nb [2], Ti [14], and V [15] as interlayer materials. Though such sandwich design reduces the stress concentration and suppresses direct reaction between both parent metals, which promotes the formation of brittle intermetallic phase FeW and metal carbides [9], the single metal interlayer itself may react with one or both of the parent metals to form new intermetallic compounds or other brittle phases. Thus the joint quality is still necessary to be improved.

This paper aims to demonstrate the feasibility of diffusion bonding of W to steel with V/Ni composite interlayer, which can reduce or avoid the formation of hard and brittle phases in the joint. And the focus is placed on the interfacial microstructure and mechanical properties of the W/V/Ni/steel bonded joints.

2. Experimental Procedure

Commercially available pure W (99.95% purity) and Fe–17Cr ferritic stainless steel with the dimensions of 16 mm diameter and 13 mm length were used in this study. V and Ni foils were used as insert metals, each of which has the purity of 99.95% and thickness of 0.2 mm and 0.1 mm, respectively.

Prior to diffusion bonding, the mating surface of all materials was prepared by conventional grinding techniques with final grinding on #1500 emery paper. The materials were then cleaned in an ultrasonic bath using acetone for 15 min and finally dried in air. The prepared materials, assembled in the structure of W/V/Ni/steel as shown in Fig. 1, were mounted in a graphite mold. Diffusion bonding of the assembly was performed at 1050 °C for 1 h in a hot-pressing furnace at a heating rate of 10 °C/min in vacuum ($<10^{-3}$ Pa). Uniaxial load of 10 MPa was applied along the longitudinal direction of the sample. Once the bonding process was completed, the load was removed, and the joints were cooled at a rate of 5 °C/min to 400 °C and followed by furnace cooling in vacuum to room temperature (RT).

The cross-sections of the diffusion bonded joints were cut perpendicularly to the joining interface and were prepared for metallographic examination by standard polishing techniques up to 1 μm. The microstructures of the reaction layers near the diffusion bonding interface were examined in a field-emission scanning electron microscope (Nova Nano SEM230) using back-scattered mode (SEM–BSE). The distribution of various elements across the bonded zones was analyzed by energy dispersive spectroscopy (EDS) and electron probe microanalysis (EPMA, JXA8530F). The phases in the V/Ni reaction zone were determined by X-ray diffraction (XRD, D/MAX-2550) with Cu Kalpha radiation. The mechanical properties of the W/V/Ni/steel joints were evaluated by hardness and tensile tests. The hardness across the bonding interface was determined by a nanohardness tester (VNHT) with a load of 30 mN. The room temperature tensile strengths of the joints were evaluated by a tensile testing machine (Instron-3369) at a crosshead speed of 1 mm/min. The interlayer was at the center of the gauge length. Fracture surfaces of the samples were observed in secondary electron mode of SEM using EDS to reveal the nature and location of failure under loading.

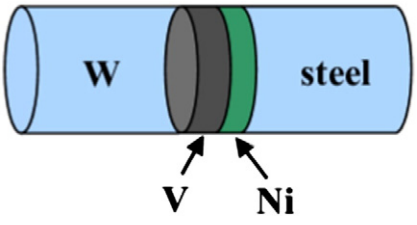

Fig. 1 – Schematic representation of the sample assembly.

3. Results and Discussion

3.1. Microstructural Characterization

The SEM–BSE images of W/V/Ni/steel bonded joints are given in Fig. 2. It has been observed that the diffusion bonding of W to steel was successful. No unbounded regions and no micro-cracks could be found along the bond interfaces of steel/Ni, Ni/V, and V/W. At low magnification of SEM–BSE, atoms from the substrates and insert materials (Ni, V) diffused continuously toward each other during the diffusion bonding. The steel/Ni and V/W interfaces are planar in nature and thin diffusion layers were revealed. The Ni/V interface is characterized by the presence of a light shaded reaction zone which has been observed.

3.1.1. Steel/Ni Interface

The interfacial microstructures of the steel/Ni diffusion interface of the bonded samples are shown in Fig. 3. Although interdiffusion occurred, neither intermediate phases nor reaction products were observed, at least within the resolution limit of SEM–BSE, as shown in Fig. 3(a). This is attributed to the good compatibility between Ni and steel. In order to determine the elemental distribution and migration behavior, EPMA line-scan was performed for the elements of interest in the joint. Fig. 3(b) is the EPMA elemental concentration profiles across the steel/Ni interface. It reveals the diffusion traces of element Fe, Cr and Ni, from which it can be noted that Fe, Cr and

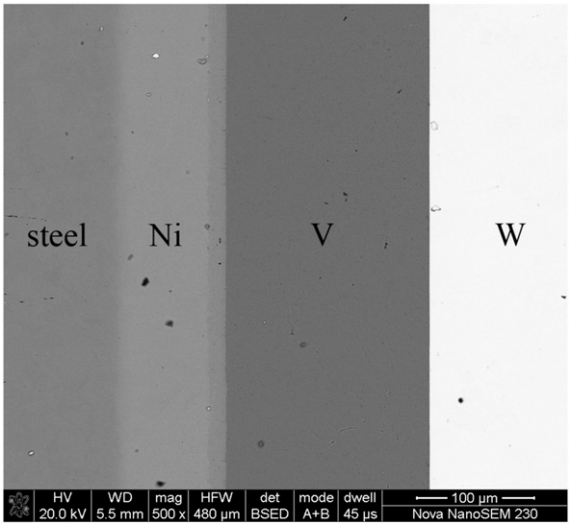

Fig. 2 – SEM–BSE images of the cross-section of W/steel joint bonded.

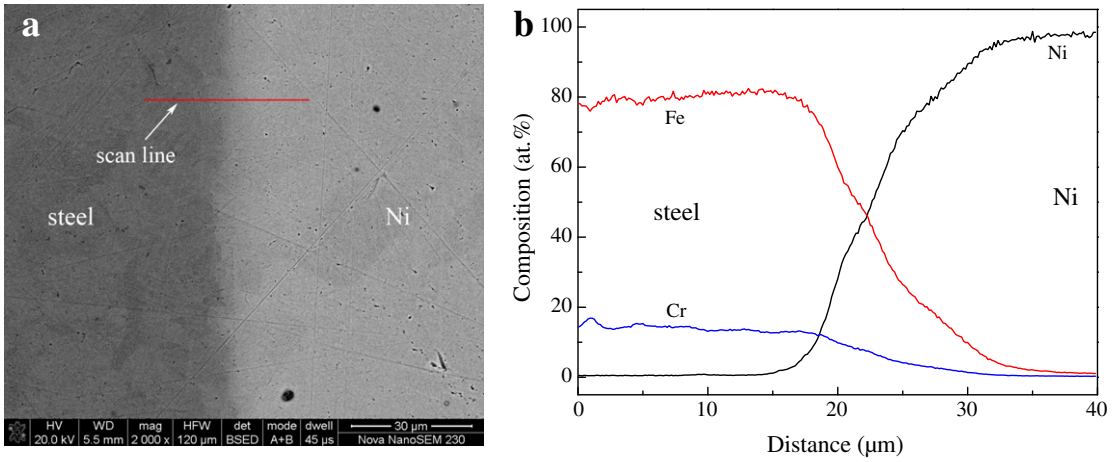

Fig. 3 – Back-scatter electron micrograph and EPMA elemental concentration profile of the diffusion bonded joint at the steel/Ni interface.

Ni concentrations change smoothly in the diffusion zone, which indicates the absence of intermetallic compounds but solid solution formation. This is consistent with the Ni–Fe and Ni–Cr phase diagrams [16].

3.1.2. *Ni/V Interface*

Fig. 4 shows the SEM–BSE micrograph of the Ni/V interface of the joints with EPMA line scanning to show the concentration profiles of the elements. It can be recognized from the color contrast that a diffusion zone was formed between Ni and V (shown in Fig. 4(a)). The Kirkendall voids were formed in the diffusion zone due to the imbalance in flux transfer of Ni and V atoms during diffusion bonding [17]. In addition, a few transverse cracks were also observed in the diffusion zone near the V side. The formation of these cracks may be attributed to the following reasons: (1) the CTE mismatch between W and steel (4.5×10^{-6} 1/K for W and 12–14×10^{-6} 1/K for steel [12]); (2) the CTE mismatch between Ni and V (13.3×10^{-6} 1/K for Ni and 8.3×10^{-6} 1/K for V); and (3) the strong diffusion reaction between Ni and V. The residual stress formed in the diffusion zone due to the CTE mismatch is responsible for the formation of cracks. However, considering that crack was not observed in other regions of the diffusion zone, the CTE mismatch on the crack formation is not believed to be the main factor. One possible explanation is the strong interaction between Ni and V. According to the literature [14,18], the mismatch of atomic sizes of bonded materials may lead to cracking at the joining interface. However, the atomic radius of Ni is close to that of V, and the two elements are similar in atomic structure and electron shell structure. So the crack formation may be caused by the formation of brittle intermetallic compounds in the diffusion zone, see the after presented hardness test results (Section 3.2.2). This justification, however, does not exclude the effect of CTE mismatch between W and steel and between Ni and V, because the CTE mismatch may lead to large residual stress in the joints after bonding.

Fig. 4(b) reveals the diffusion traces of elements Ni and V, from which a diffusion layer with a thickness of about 20 µm can be found. It should be noted that, compared with the diffusion traces of elements Fe, Cr and Ni in Fig. 3(b), there existed several plateau in the element dispersion curve, which indicated that several kinds of intermediate phases

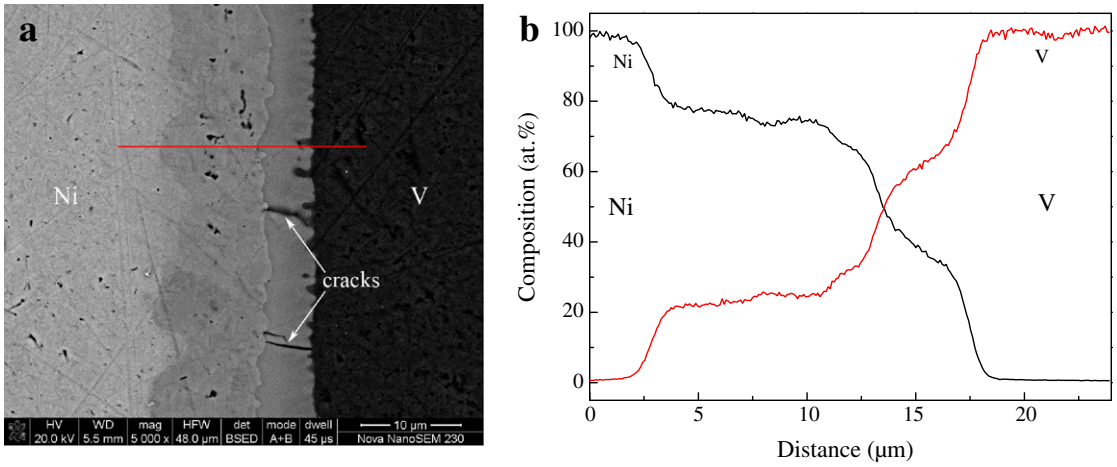

Fig. 4 – SEM–BSE micrograph and EPMA elemental concentration profile of the diffusion bonded joint at the Ni/V interface.

were formed in the diffusion layer. In order to determine the phase distribution and the possible presence of reaction products, EPMA elemental maps and quantitative elemental concentration profile were applied for the elements of interest in the diffusion zone, as shown in Fig. 5. Different Ni–V phases can be identified as diffusion layers formed between Ni and V through the variation of the intensities of the EPMA signals. The diffusion layer appears to consist of six sub-layers, as shown from the elemental maps in Fig. 5(a). Sub-layer A and Sub-layer F show a gradual change of element distribution of Ni and V, whereas in other sub-layers, Ni and V are homogeneously distributed, respectively. The phase boundary and the phase constitutes of can be recognized from the EPMA quantitative elemental concentration profiles. In Fig. 5(b), four sharp increases in the V concentration were clearly noted at the point corresponding to the phase boundary between layers. This means that there are four intermediate phases formed in the diffusion zone.

From the quantitative elemental analysis in Fig. 5(b), the reaction phases of the sub-layers in the diffusion zone can be predicted according to the Ni–V binary phase diagram [16], and the corresponding EPMA chemical composition analysis results of these layers are listed in Table 1. Ni-rich solid solution (Ni(V)), Ni_3V, Ni_2V, Ni_2V_3, NiV_3, and V-rich solid solution (V(Ni)) are present in Sub-layers A, B, C, D, E, H and F, respectively. The thickness of the different Ni–V base intermetallic compounds can be seen from the EPMA analysis (Fig. 5(b)). It is found that the thickness of Ni_3V and Ni_2V_3 layers is larger than that of Ni_2V and NiV_3 layers. As far as the growth behavior of compound layers for a specific alloy system is concerned, an intermetallic compound with a lower melting point T_m will grow faster than that with a higher T_m, as demonstrated by Zhong et al. [13]. In the present Ni–V system, Ni_3V and Ni_2V_3 have higher melting points compared to Ni_2V and NiV_3. On the contrary, the thickness of Ni_3V and Ni_2V_3 layers is larger, indicating that T_m is not the rate-controlling process for the growth rate of intermetallic lays in the present study. The large thickness of Ni_3V or Ni_2V_3 layers may be attributed to the large composition range of Ni_3V and Ni_2V_3. According to the literature date [16,19], the Ni–V series alloys have a common property, that is, the composition of each compound is within a certain range. Larger composition range may benefit the nucleation and/or growth of the intermetallic phases. So, the thickness of Ni_3V and Ni_2V_3 layers being larger, rather than that of Ni_2V or NiV_3 layers, is reasonable.

Table 1 – EPMA analysis results of layers A–F in Fig. 5(b).

Reaction layer	Chemical composition (at.%)		Phase
	Ni	V	
A	87.6–100	0–12.4	Ni-rich solid solution
B	74.5–79.3	20.7–25.5	Ni_3V
C	66.6–67.3	32.7–33.4	Ni_2V
D	28.8–42.8	57.4–71.2	Ni_2V_3
E	~22.9	~77.1	NiV_3
F	0–3.3	96.7–100	V-rich solid solution

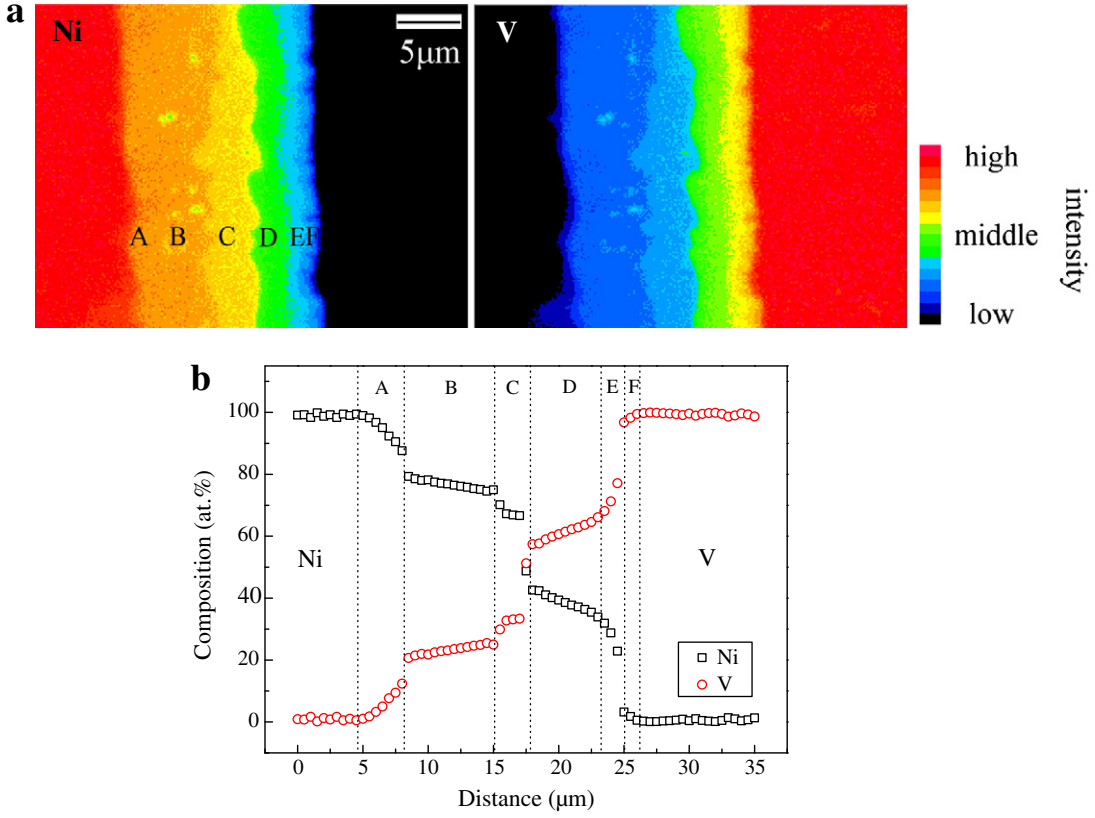

Fig. 5 – EPMA elemental maps and quantitative elemental concentration profile of Ni and V in the diffusion zone.

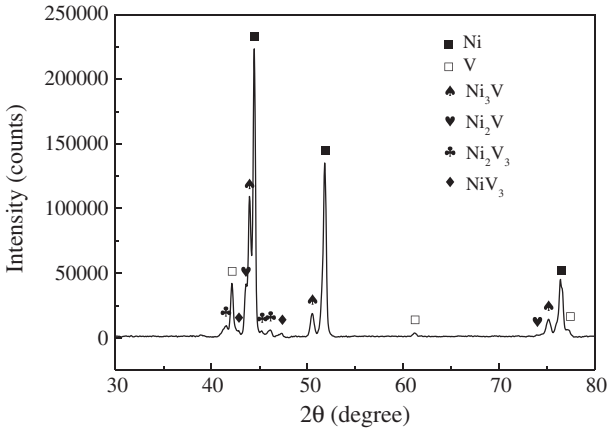

Fig. 6 – X-ray diffraction pattern measured on the cross-section of Ni/V interface.

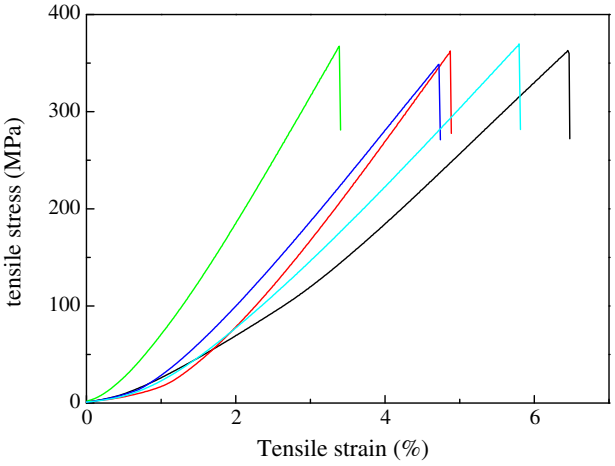

Fig. 8 – Tensile curve of the W/V/Ni/steel joints.

In order to characterize the reaction products at the Ni/V interface, the cross-sections of the joint bonded were analyzed by XRD, and the XRD pattern is shown in Fig. 6. The XRD analysis confirms the presence of different intermetallic compounds like Ni_3V, Ni_2V, Ni_2V_3 and NiV_3 in the diffusion zone.

3.1.3. *V/W Interface*

The SEM–BSE micrographs and EPMA concentration profiles of the V/W interface of the diffusion bonded samples are shown in Fig. 7. From the SEM–BSE images (Fig. 7(a)), the interface region is clearly visible. Note that there are many small white contrasts in the V, which may be the distribution of W on the grain boundaries of V as a result of W diffusion into V. By the EPMA, a layer of about 2.5 μm thick, which was identified to be a V–W solid solution (Fig. 7(b)), was formed between V and W. The absence of intermetallic compounds in the diffusion zone is indicated by the smoothly varying nature of the profile curves. This observation can be rationalized on the basis of their mutual solubility from the V–W binary phase diagram. It should be noted that, compared with the steel/Ni interface, the diffusion layer thickness by EPMA analysis is very thin, which was also observed by Basuki and Aktaa [15]. This may be attributed to the high melting temperature of W and V (~3696 K for W and ~2193 K for V), especially W element. Solid state diffusion bonding processes are usually conducted at temperatures in the range of 0.5–0.8 T_m (K). The optimal temperature for diffusion bonding of W in vacuum is found about 0.67 T_m (2200 °C) [20]. This means that the bonding temperature at 1050 °C is too low for the diffusion of tungsten, e.g. the vacancy diffusion mechanisms of W are not activated [9].

3.2. *Mechanical Characterization*

3.2.1. *Tensile Strength Evaluation and Fractured Surface Observation*

The strength and reliability of W/steel joints are of importance for applications. The strength of the joints was evaluated by tensile tests at room temperature, and the bonded specimen possesses a relatively high strength of ~362 MPa (Fig. 8). The spread of strength values observed for the joints was probably credited to the spread on the strength level of the W itself, owing to its brittle nature and sensitivity of impurity

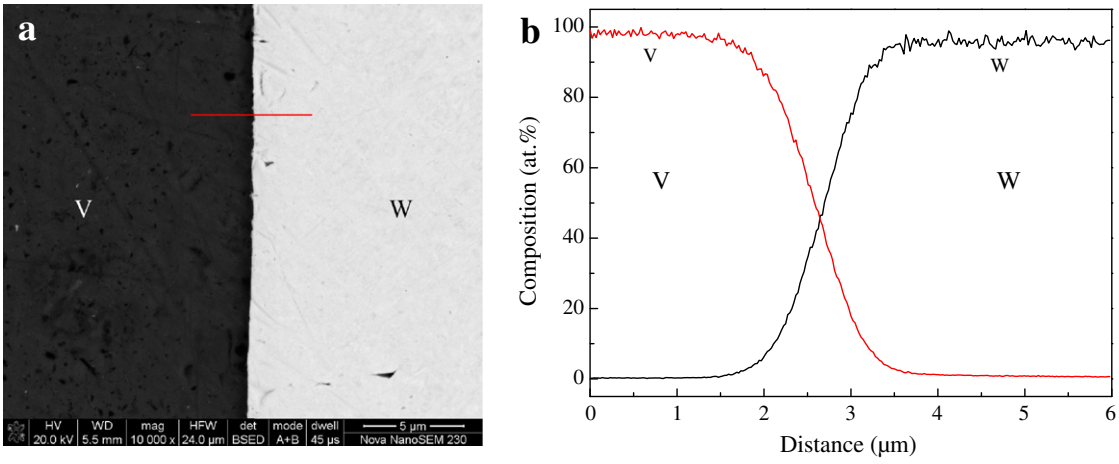

Fig. 7 – SEM–BSE micrograph and EPMA elemental concentration profile of the diffusion bonded joint at the V/W interface.

distribution. Fig. 9 shows the SEM images of fracture surface on the W side of the joint bonded after tensile test. Although brittle intermetallic compounds Ni_3V, Ni_2V, Ni_2V_3 and NiV_3 were formed at the Ni/V interface, all the joints failed predominantly in W near the joining interface during tensile tests. The reason for this phenomenon may be due to the residual stress induced by the CTE mismatch in the W/steel joints. The contractions of the W, V, Ni and steel during cooling from the joining temperature are different since they have inherently different CTE, which results in the residual stress in the joint. In addition, the formation of new phases in the diffusion zone (especially for the Ni_3V, Ni_2V, Ni_2V_3 and NiV_3), which have different CTE, may lead to residual stress in the joints after joining.

The maximum residual stress, which is usually located in low CTE material near to the joining interface, as demonstrated by most authors [21–23], plays an important role in determining the mechanical behavior of dissimilar material joints. Jadoon et al. [24] tried Cu and Ti/Cu/Ti as inserted materials for diffusion bonding of silicon nitride to Fe cr alloy, and they found that the thermal stresses that are induced in the silicon nitride was the main reason for failure in the ceramic during rigorous thermal cycling. Furthermore, Kalin et al. [5] established a model of the distribution of normal thermal stress in a brazed W/steel joint by theoretical calculation and experiment, and confirmed that the equivalent tensile stress had a maximum in a less ductile material (W) at some distance from the joint. In this work, the CTE mismatch between W and V resulted in residual stress in W near V/W interface. In addition, the residual stress induced by CTE mismatch between V and Ni and between Ni and steel may partly transfer to W near W/V interface because the V and Ni interlayers were thin [25]. Therefore, the maximum residual stress in the W/steel joint was expected to be presented in W near W/V interface, and cracking in W near W/V interface is highly possible when the joint was subjected to a tensile load. Indeed, most of the joints fractured in W near the V/W interface.

As it can be seen in Fig. 9, the fracture surface is macroscopically divided into two regions, I and II. Region I is the torn-off W that remained on the fracture surface, as displayed in Fig. 9(a). The fraction of W that remained on the fracture surface is larger than that of region II. This allows us to deduce that the W side near the V/W interface is subjected to large residual stress. The fractured surface is characterized by the appearance of the faceted grains, suggesting that the joints failed in an intergranular (in W) and transgranular (in region II) mode. In addition, some micro-cracks and micro-sized pores (as shown by arrows) were also found on the fracture surface.

Fig. 9(b) and (c) shows the typical fractured surfaces of region II. Some phases on the facture surfaces were identified as containing W, V and Ni by EDS. Taking into account the microstructures of the cross-section of Ni/V and V/W interfaces

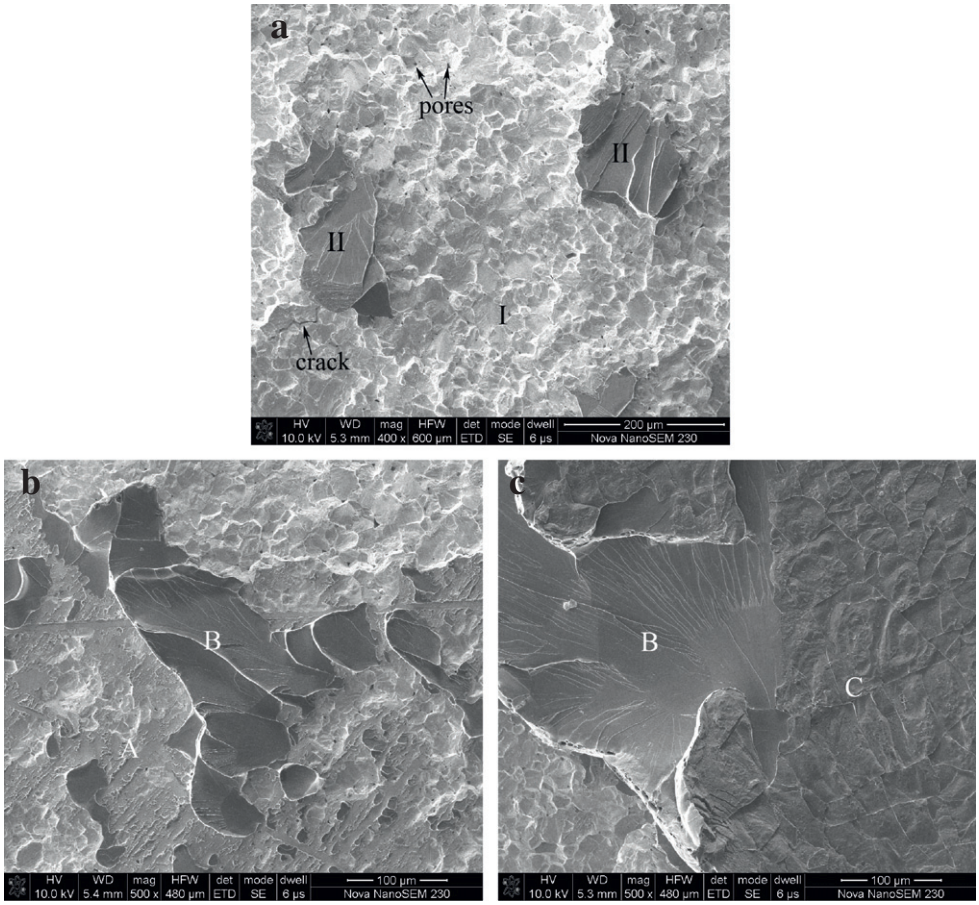

Fig. 9 – Fracture surface of the W/V/Ni/steel joint bonded after tensile test. The fracture on the W side is divided into regions I and II. (a) Representative fractured surface, (b) and (c) the different fracture surfaces of region II.

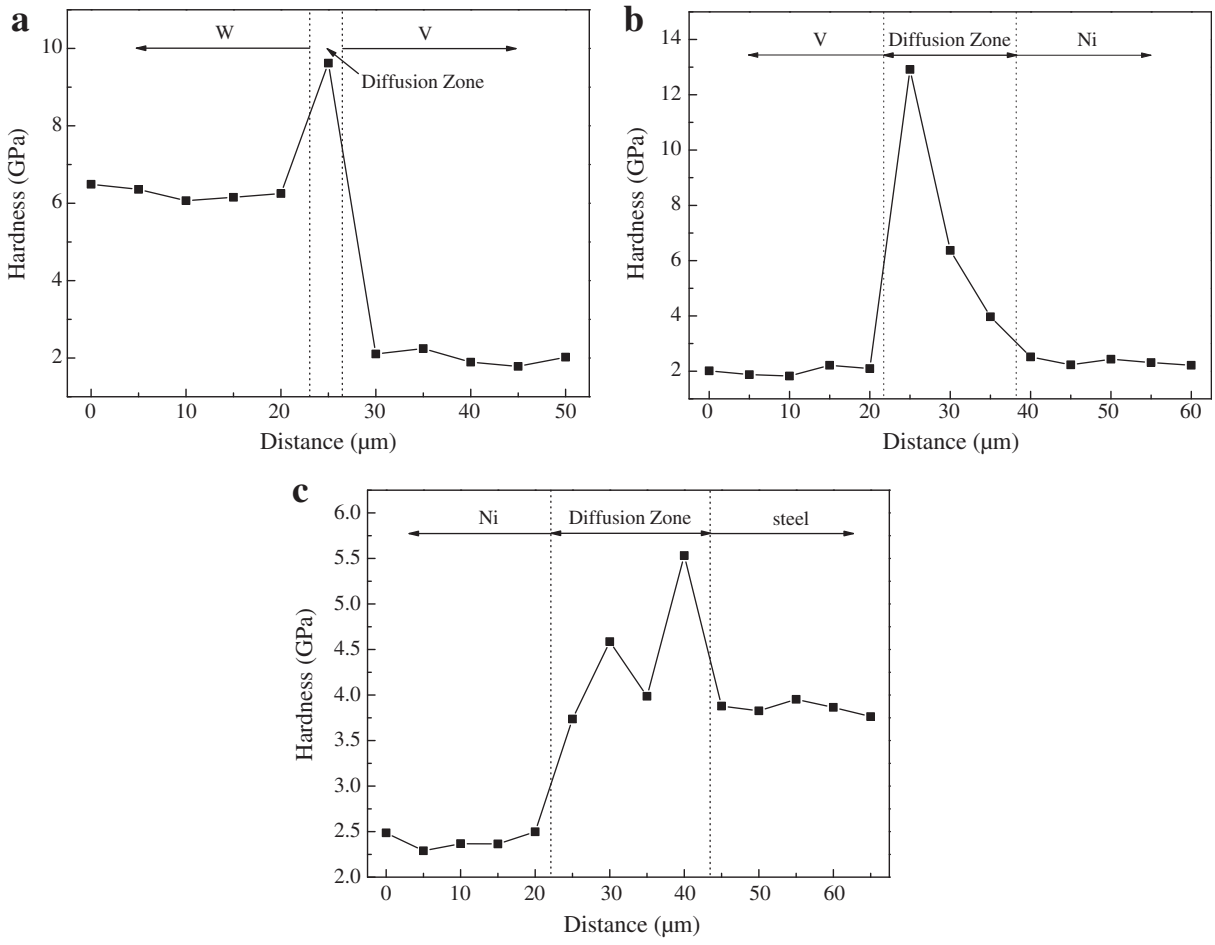

Fig. 10 – Hardness distribution along the cross-section of (a) W/V, (b) V/Ni, and (c) Ni/steel interfaces, respectively.

in Figs. 4 and 7, one can infer that region II corresponds to the V and the diffusion zone of Ni/V and V/W. The average composition of the area A is W (~48 at.%) and V (~52 at.%), suggesting the existence of V–W solid solution. The cleavage facets (area B) is V with a composition of V (nearly 100 at.%).

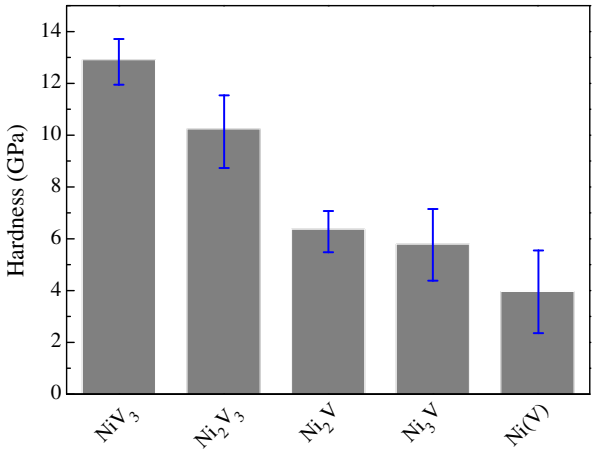

Fig. 11 – Nanohardness values of reaction products in the diffusion zone of Ni/V interface.

While area C is comprised of Ni (~32 at.%) and V (~68 at.%), intermetallic phases (especially the Ni_2V_3) can be expected in this area. Therefore, the failure behavior of the bonded joints during tensile tests can be explicated that the crack initiated in W near the V/W interface due to the residual stress concentration and then propagated rapidly along the W grain boundaries and into V–W diffusion zone, V and Ni–V intermetallic phases.

In the previous attempt, Ni and V have been used separately as an interlayer material to produce the W/steel transition joints and achieved the tensile strength of about 215 and 207 MPa at RT, respectively [13,15]. Compared with them, the W/V/Ni/steel joint with a higher strength was produced in this work, which can be attributed to the beneficial effects on reducing the residual stresses and minimizing the brittle intermetallic compound formation between bulk material and interlayer by the design of V/Ni composite interlayer.

3.2.2. *Hardness Distribution Across the Interfaces*

The micro-mechanical properties of ceramic/metal and metal/metal bonded interfaces can be evaluated by nano-indentation tests, which are useful techniques to evaluate the mechanical properties of either films or small volumes of materials. The hardness was evaluated on the polished cross-section of the

joint at the W/V, V/Ni and Ni/steel interfaces. Fig. 10(a) through (c) shows the variation in hardness across profiles of the W/V (from W to V), V/Ni (from V to Ni), and Ni/steel (from Ni to steel) interfaces, respectively. It can be seen that substantial changes were observed at the interfaces which are directly related to the composition and thickness of diffusion zones generated. At the W/V interface, the high hardness values (~9.6 GPa) observed in the diffusion zone is associated with the interdiffusion of W and V. In the diffusion zone of Ni/V interface, similarly, a higher hardness was noted in comparison with the Ni or steel, which is the evidence of Fe and Cr penetration into the Ni interlayer, and Ni penetration into steel. Likewise, the high hardness values (3–13 GPa) were observed in the diffusion zone between Ni and V, which clearly indicate the formation of intermetallic compounds. The nanohardness values of reaction products in the diffusion zone of Ni/V interface are shown in Fig. 11. The hardness of V(Ni) cannot be evaluated because its volume fraction is too small in the diffusion zone. The maximum hardness value of ~12.9 GPa was obtained for NiV_3, which was six times higher than the hardness of V. Next to NiV_3, the Ni_2V_3 shows a high hardness value that is slightly lower than that of NiV_3. Considering the whole bonded specimen, the NiV_3 and Ni_2V_3 phases can be considered as the hardest region and there should be the weakest region against the residual stress in the joint after bonding, which is the reason for the crack formation near the V side in the diffusion zone of the Ni/V interface (see Fig. 4(a)).

This observed region-dependent hardness is ascribed to the solid solution strengthening effect and intermetallic compound formation, which are related to the reaction and interdiffusion process. These results are further evidence of the interdiffusion of W and V, Ni reaction with V, and Fe and Cr atom penetration into Ni and Ni penetration into steel.

4. Conclusions

The proposed V/Ni composite interlayer was successful for diffusion bonding of W to steel. The interfacial microstructure and mechanical properties of the bonded specimen have been investigated and the following conclusions were drawn:

(1) Microstructure analysis indicated that a good bonding at the W/V, V/Ni and Ni/steel interfaces was informed. Ni_3V, Ni_2V, Ni_2V_3 and NiV_3 were identified by EPMA and XRD at the Ni/V interface, whose formations are attributed to the strong interaction between Ni and V. On the other hand, smooth changes in elemental concentrations across the W/V and Ni/steel interfaces demonstrated that it was devoid of intermetallic phases.
(2) The tensile strength of the as-bonded W/steel joints is about 362 MPa, which is comparable with that of the joints obtained by using Ni or V interlayer. All specimens always fractured in W near the V/W interface which is the maximum residual stress concentration region in the joints, during tensile tests, in a brittle fracture mode.
(3) The observed region-dependent hardness at various interfaces is associated to the strengthening effect of solid solution and formation of intermetallic compounds.

Acknowledgments

The authors gratefully acknowledge the financial support from the National Natural Science Foundation of China (No. 50774098), the National 863 Plan Project of China, and the Program for “Chang Jiang Scholars” in University of Ministry of Education of China.

REFERENCES

[1] Norajitra P, Giniyatulin R, Holstein N, Ihli T, Krauss W, Kruessmann R, Kuznetsov V, Mazul I, Ovchinnikov I, Zeep B. Status of He-cooled divertor development for DEMO. Fusion Eng Des 2005;75–79:307–11.
[2] Basuki WW, Aktaa J. Investigation of tungsten/EUROFER97 diffusion bonding using Nb interlayer. Fusion Eng Des 2011;86:2585–8.
[3] Klueh RL, Gelles DS, Jitsukawa S, Kimura A, Odette GR, Van der Schaaf B, Victoria M. Ferritic/martensitic steels—overview of recent results. J Nucl Mater 2002;307–311:455–65.
[4] Kalin BA, Fedotov VT, Sevrjukov ON, Kalashnikov AN, Suchkov AN, Moeslang A, Rohde M. Development of brazing foils to join monocrystalline tungsten alloys with ODS-EUROFER steel. J Nucl Mater 2007;367–370:1218–22.
[5] Kalin BA, Fedotov VT, Sevrjukov ON, Moeslang A, Rohde M. Development of rapidly quenched brazing foils to join tungsten alloys with ferritic steel. J Nucl Mater 2004;329–333:1544–8.
[6] Chehtov T, Aktaa J, Kraft O. Mechanical characterization and modeling of brazed EUROFER-tungsten-joints. J Nucl Mater 2007;367–370:1228–32.
[7] Oono N, Noh S, Iwata N, Nagasaka T, Kasada R, Kimura A. Microstructures of brazed and solid-state diffusion bonded joints of tungsten with oxide dispersion strengthened steel. J Nucl Mater 2011;417:253–6.
[8] Noh S, Kasada R, Oono N, Nagasaka T, Kimura A. Joining of ODS steels and tungsten for fusion applications. Mater Sci Forum 2010;654–656:2891–4.
[9] Basuki WW, Aktaa J. Investigation on the diffusion bonding of tungsten and EUROFER97. J Nucl Mater 2011;417:524–7.
[10] Kundu S, Chatterjee S. Interface microstructure and strength properties of diffusion bonded joints of titanium–Al interlayer–18Cr–8Ni stainless steel. Mater Sci Eng A 2010;527:2714–9.
[11] He P, Feng JC, Zhang BG, Qian YY. A new technology for diffusion bonding intermetallic TiAl to steel with composite barrier layers. Mater Charact 2003;50:87–92.
[12] Zhong ZH, Jung H, Hinoki T, Kohyama A. Effect of joining temperature on the microstructure and strength of tungsten/ferritic steel joints diffusion bonded with a nickel interlayer. J Mater Process Technol 2010;210:1805–10.
[13] Zhong ZH, Hinoki T, Kohyama A. Effect of holding time on the microstructure and strength of tungsten/ferritic steel joints diffusion bonded with a nickel interlayer. Mater Sci Eng A 2009;518:167–73.
[14] Zhong ZH, Hinoki T, Nozawa T, Park YH, Kohyama A. Microstructure and mechanical properties of diffusion bonded joints between tungsten and F82H steel using a titanium interlayer. J Alloys Compd 2010;489:545–51.
[15] Basuki WW, Aktaa J. Diffusion bonding between W and EUROFER97 using V interlayer. J Nucl Mater 2012;429:335–40.
[16] Nayeb-Hashmi AA, Clark JB. Binary alloy phase diagrams. 2nd ed. Materials Park, OH: ASM International; 1991.

[17] Sabetghadam H, Zarei Hanzaki A, Araee A. Diffusion bonding of 410 stainless steel to copper using a nickel interlayer. Mater Charact 2010;61:626–34.
[18] Yilmaz O, Aksoy M. Investigation of micro-crack occurrence conditions in diffusion bonded Cu-304 stainless steel couple. J Mater Process Technol 2002;121:136–42.
[19] Wang Z, Zhou H, Wang Z, Yao Q. The 773 K isothermal section of the Nd–Ni–V ternary system. J Alloys Compd 2008;458:425–7.
[20] Kazakov NF, Kvasnitsky VF. Bonding of refractory and active metals and their alloys. In: Kazakov NF, editor. Diffusion bonding of materials. Mir Publisher; 1985.
[21] Conzone SD, Butt DP, Bartletta H. Joining MoSi2 to 316L stainless steel. J Mater Sci 1997;32:3369–74.
[22] Shirzadi AA, Zhu Y, Bhadeshia HKDH. Joining ceramics to metals using metallic foam. Mater Sci Eng A 2008;496:501–6.
[23] Xiong HP, Mao W, Xie YH, Guo WL, Li XH, Cheng YY. Brazing of SiC to a wrought nickel-based superalloy using CoFeNi(Si, B)CrTi filler metal. Mater Lett 2007;61:4662–5.
[24] Jadoon AK, Ralph B, Hornsby PR. Metal to ceramic joining via a metallic interlayer bonding technique. J Mater Process Technol 2004;152:257–65.
[25] Martinelli AE, Drew RAL, Fancello EA, Rogge R, Root JH. Neutron diffraction and finite-element analysis of thermal residual stresses on diffusion-bonded silicon carbide–molybdenum joints. J Am Ceram Soc 1999;82:1787–92.